

Article

Rapid and precise measurement of the hydrogen isotope composition of phyllosilicates by continuous flow OA-ICOS

John A. Mering, and Shaun L. L. Barker

Anal. Chem., **Just Accepted Manuscript** • DOI: 10.1021/acs.analchem.7b04992 • Publication Date (Web): 20 Jan 2018

Downloaded from <http://pubs.acs.org> on January 20, 2018

Just Accepted

"Just Accepted" manuscripts have been peer-reviewed and accepted for publication. They are posted online prior to technical editing, formatting for publication and author proofing. The American Chemical Society provides "Just Accepted" as a free service to the research community to expedite the dissemination of scientific material as soon as possible after acceptance. "Just Accepted" manuscripts appear in full in PDF format accompanied by an HTML abstract. "Just Accepted" manuscripts have been fully peer reviewed, but should not be considered the official version of record. They are accessible to all readers and citable by the Digital Object Identifier (DOI®). "Just Accepted" is an optional service offered to authors. Therefore, the "Just Accepted" Web site may not include all articles that will be published in the journal. After a manuscript is technically edited and formatted, it will be removed from the "Just Accepted" Web site and published as an ASAP article. Note that technical editing may introduce minor changes to the manuscript text and/or graphics which could affect content, and all legal disclaimers and ethical guidelines that apply to the journal pertain. ACS cannot be held responsible for errors or consequences arising from the use of information contained in these "Just Accepted" manuscripts.



ACS Publications

Rapid and precise measurement of the hydrogen isotope composition of phyllosilicates by continuous flow OA-ICOS

John A. Mering^{1*}, Shaun L. L. Barker¹

¹School of Science, University of Waikato, Hamilton, 3240, New Zealand

*Corresponding author: johnmering@gmail.com

ABSTRACT: New methodology is presented for analyzing hydrogen isotope ratios (D/H) in phyllosilicate minerals by laser absorption spectroscopy. D/H measurements were carried out using an OA-ICOS instrument operated in a continuous flow configuration. Water was extracted from minerals in a high temperature quartz column and advanced to the analyzer in a dry air carrier gas stream. We report the first D/H measurements by a laser system for serpentine, muscovite, sericite, talc, and biotite. We also measure kaolinite, gypsum, and small volumes of water. Materials, excluding biotite, were calibrated to within 1.5 ‰ of IRMS-measured δD_{VSMOW} values, with an average precision of 1.1 ‰. Biotite δD measurements were up to 10 ‰ more positive than established IRMS values, due to partial reduction of evolved waters by Fe in the high temperature column. We provide recommendations for overcoming redox interference for measurements of biotite, and other ferrous materials, by OA-ICOS. Rapid, precise, and accurate analyses were carried out on water volumes as low as 0.25 μ L extracted from minerals. With the exception of talc, the time required for thermal dewatering and measurement is 140 seconds, which translates into a throughput of up to 6 mineral samples per hour, including replicates. By demonstrating high precision, rapid throughput, low cost, and ease of operation, we provide a tool that should enable researchers at institutions with limited funding to routinely measure D/H in hydrous minerals. The protocols presented herein should also be useful to commercial users seeking to produce high density isotope datasets relevant to exploration of hydrothermal ore deposits and geothermal fields.

INTRODUCTION

Hydrogen stable isotope signatures in minerals provide a means to reconstruct fluid history in both surficial and subsurface deposits of geologic and environmental interest. Historically, a number of workers have measured D/H signatures in clays, micas and serpentine minerals to study fluid flow in hydrothermal settings.¹⁻¹⁰ Hydrogen isotope values in minerals are routinely measured in both active²⁻⁶ and ancient hydrothermal environments,^{1,3,8-10} to map fluid flow and temperature gradients.⁷⁻⁹ Important settings for these investigations encompass modern geothermal fields,²⁻⁴ submarine spreading centers,⁵⁻⁶ ancient hydrothermal ore deposits,^{1,3,8-10} and sedimentary basins.¹¹⁻¹² From an economic standpoint, these systems are relevant to geothermal energy development,⁴ mineral deposit studies,^{3,8-10} and hydrocarbon exploration.¹¹⁻¹² Collectively, researchers in these fields have benefitted from advances in stable isotope measurement technology over the last 60 years.¹³ Yet, despite improvements in speed, precision, and accuracy,¹⁴⁻¹⁶ costs of hardware and consumables associated with Isotope Ratio Mass Spectrometry (IRMS) remain high.¹⁷ In this paper, we demonstrate that continuous flow Off-Axis Integrated Cavity Output Spectroscopy (OA-ICOS) is a viable, lower cost, platform for rapidly quantifying D/H ratios in hydrous minerals.

Although Laser Absorption Spectroscopy (LAS) instruments, including OA-ICOS, are now widely used for isotopic measurement of water samples,¹⁸⁻¹⁹ they are rarely utilized to measure hydrous solids. LAS manufacturers do not provide “off the shelf” sample preparation systems for rapidly extracting water from hydroxyl bearing minerals, and other solids (e.g. organic compounds). Data handling software, for processing and calibrating results is also not available at this time. Consequently, work utilizing LAS to measure D/H in solid materials has been largely relegated to proof of concept papers. Trial work has focused on measurements of gypsum,²⁰⁻²³ fluid inclusions,²⁴ organic compounds,²⁵ and several clays,²⁶ in which water was extracted either offline,²⁰⁻²³ or in continuous flow.²⁴⁻²⁶ A recent Cavity Ringdown Spectroscopy (CRDS) protocol enables interpretation of isotope signals across slowly evolved water peaks in gypsum and clay minerals.²⁶ However, complex hardware, and processing times of 90 minutes for clays, render the technique less useful for applications in which high sample throughput is required.

Herein, we provide documentation of a methodology that enables routine measurement of D/H ratios of hydrous minerals using readily available and reliable equipment. A comprehensive discussion of hardware operation and data processing is provided to enable users of laser absorption spectrometers to rapidly analyze, and accurately calibrate, D/H signals in minerals. Measurements were performed using a Los Gatos Research (LGR) OA-ICOS analyzer (San Jose, CA, USA),²⁷ but the principles described here should be applicable to users of other LAS systems, including CRDS. Tests were carried out on common hydrous minerals, including serpentine, muscovite, sericite, kaolinite, talc, biotite, and gypsum. The analytical setup described here is characteristically simpler than Thermal Conversion Elemental Analysis (TC/EA) IRMS systems, but still capable of delivering precise and rapid D/H measurements.

METHODS

Hardware setup

Isotopic analyses were conducted using a LGR OA-ICOS Triple Isotope Water Vapor Analyzer (T-WVIA 45-EP), and a custom-built sample preparation line at the University of Waikato, Hamilton, New Zealand. Minerals are dewatered in a high temperature column, and the resulting water vapor pulse is transferred to the optical cell in the analyzer in a dry air carrier gas stream. A pressurized dry air cylinder was used as the carrier gas source, but any dry and oil free compressed air source would be suitable. The OA-ICOS instrument, contains a high finesse optical cell, which operates on the principle of cavity enhanced absorption. The analyzer is described in literature.^{17-19,25,27-29} Measurement is accomplished by introducing H₂O vapor into the cell, which contains highly reflective mirrors, a diode laser, and photodetector. The laser is pulsed through the cell, and the absorption spectra of water isotopologues are measured. Mixing ratios for H₂¹⁶O, HDO, H₂¹⁸O, and H₂¹⁷O are calculated from absorption spectra, and corrected to account for cavity temperature, pressure, laser path length, and ringdown time.^{17-19,25,27-29} Concentrations of isotopologues were measured in parts per million by volume (ppmv) at 1 Hz.

The mineral dehydration line, depicted in Figure 1, was designed to facilitate high sample throughput and minimize memory. The dehydration line features a high temperature quartz column, emplaced in a Carbolite (Hope, UK) tube furnace, paired with a Costech Zero Blank (Valencia, CA, USA) carousel autosampler. The autosampler is triggered using an Arduino (Somerville, MA, USA) single-board microcontroller, which generates a 1 second contact closure. A USB access port on the controller allows users to adjust the timing of the autosampler drop interval. Mineral powders are dewatered in the column, at temperatures between 950 and 1000 °C. For straightforward maintenance, a quartz liner was installed to sequester used capsules and mineral powder. The liner rests upon 3 indentations in the hottest interval of the quartz column. The base of the liner is closed, and the wall of the liner is perforated to allow the flow of water vapor and carrier gas through to the analyzer. Plugs of quartz wool and silver wool are emplaced at the base of the column to preclude the transit of mineral powder, and sulfur-bearing compounds, into the analyzer. No other packing (e.g. quartz chips, Cr₂O₃) was utilized. A pair of 2-μm and 0.5-μm filters (Valco Instruments Co., Inc., USA) were installed below the column, upstream of the OA-ICOS unit, to prevent clogging of the internal filter in the analyzer.

During the course of the study, filters in the prep line occasionally became coated by sulfur compounds. Sulfur buildup occurred during analyses of hydrothermally altered rocks, which contained pyrite, and hydrous sulfates. This issue was mitigated by including a silver wool trap in the column packing, and by routinely changing the inline filters and quartz liner. Maintenance on the liner and filters was carried out after approximately 1 g of mineral powder had been analyzed. The filters and liner can be changed in less than 10 minutes, while the column is at normal operating temperatures. The column is connected directly to the analyzer by a 1/4 inch diameter, 75 cm long perfluoroalkoxy (PFA) tube. The tube is wrapped in heat tape, and is maintained at 95 °C during analyses.

A combination of greater heating of transfer lines, shortened transfer tubing, and a carrier gas pressure setting high enough to achieve turbulent flow resulted in the best precision and the smallest memory effect. Analysis of a synthetic gypsum sample demonstrated a reduction in memory of up to 20 percent on the first analysis in a series of replicates as a result of heating. A variety of flow and pressure settings were considered. The standard rate of carrier gas flow from the column into the optical cell is approximately 110 ml/min. Although it was possible to maintain a normal pressure of 40.3 torr (5372.9 Pa) in the OA-ICOS cell at lower flow rates, measurements of hydrogen isotope ratios were considerably less precise. At a flow setting of 60 ml/min, analytical uncertainty of δD , represented by 1 standard deviation of the mean (1 σ) of replicate measurements, was consistently greater than 5 %, and above 10 % in several cases.

In the tests reported here, the hydrogen isotope (D/H) compositions of minerals and liquid waters were measured by OA-ICOS for materials that covered an expansive range of δD_{VSMOW} values, from 0 to -189 ‰. D/H ratios were normalized to the Vienna Standard Mean Ocean Water (VSMOW) scale, using reference materials with known D/H ratios, and reported in δD notation in per mil (‰) units, unless otherwise noted.³⁰ New hydrogen isotope mineral standards were measured by TC/EA-IRMS at the University of Otago. A list of the materials evaluated by OA-ICOS in this study is provided in Table 1.

Operation

Mineral powders were weighed into 5×9 mm silver foil capsules in sets of 3 to 7 replicates. Water standards were introduced in either crimped silver capillary tubes, or as pulses delivered from the LGR manufactured Water Vapor Isotope Standard Source (WVISS) to the reaction column. Prior to analyses, powders were dried at 190 °C for 5 hours, in a vacuum oven. To limit uptake of water after drying, samples were transferred from the vacuum oven to the autosampler in heated metal trays, with a total exposure time to open air of 3 minutes or less. Up to 49 capsules may be loaded at a time, which translates into 7-16 unique samples or standards, accounting for replicates.

A typical run begins with a 4 minute dry air purge of the autosampler, followed by a 3-5 minute stabilization phase in order to achieve a background water vapor concentration of less than 250 ppmv. During stabilization, dry carrier gas flows through the autosampler, reaction tube, and analyzer. Samples are dropped into the quartz column in 140 second intervals. The throughput reported here is comparable to the measurement cycle on a continuous flow IRMS platform. Our sample throughput is significantly faster than rates reported for offline LAS measurements of gypsum hydration water,²⁰⁻²³ trial measurements of organic compounds by continuous flow OA-ICOS, where samples were dropped at 8 minute intervals,²⁵ and recent online CRDS mineral dewatering experiments.²⁶

Analyses are manifest as discreet peaks over a low background H₂O concentration. Peak maxima for 0.5 μ L water pulses liberated from minerals or water capsules were generally between 10,000 and 12,000 ppmv. The response time required for a water vapor pulse to reach the analyzer is typically 18 to 22 seconds for liquid waters in silver capillary tubes, and 20 to 30 seconds for mineral powders in silver foil capsules. The maximum water concentration in the OA-ICOS cell is attained during the first 25 seconds following the start of the peak. Recovery from the maximum water vapor concentration down to the baseline occurs more slowly. Water concentrations within the analytical cell are usually within 200 ppmv of the baseline, 70 seconds after the peak maximum. For most runs, the background vapor concentration between peaks varied by less than 100 ppmv. During standby periods between runs, the entire system is pumped down to 500 mTorr (66.7 Pa), using the internal pump on the analyzer, to preserve dry internal conditions.

Data processing

Measurements of isotopologue mixing ratios by OA-ICOS are influenced by the total H₂O vapor concentration in the optical cell. This was assessed, and corrected for, by measuring water standards over a range of concentrations, using the WVISS, as has been done in prior work.^{18-19,24-25} The WVISS is comprised of a heated nebulizer spray chamber and a dry air source. The mixing ratio of dry air and vapor from the nebulizer chamber is governed by a mass flow controller, and the pressure setting on the nebulizer spray chamber. Following the principle of identical treatment for samples and standards, the WVISS was run through the autosampler and furnace (Figure 1).³¹ Running the WVISS through the heated column is advantageous as it provides a tool for rapidly assessing column and transfer line efficiency. Positioning the WVISS upstream of the hot column also allowed for a shorter transfer line to the analyzer, which reduced intersample memory. A concentration correction example for HDO is provided in the SI.

The ratio of processed peak areas for HDO and H₂¹⁶O was applied to calculate sample D/H values, as has been done elsewhere for water isotope measurements by continuous flow LAS.²⁴⁻²⁶ Here, the trapezoidal method for peak integration was applied to HDO and H₂¹⁶O isotopologue data. Other integration techniques (i.e. Simpson's Rule) will provide δ D values that are within 0.1 ‰ of those determined by the trapezoidal method. Integration was carried out using the Peak Analyzer tool in the OriginPro® software package. Peaks were defined via a concentration trigger, with no background correction (Figure 2). A concentration threshold of 3,000 ppm H₂O was selected because the OA-ICOS analyzer does not precisely measure rare isotopologues (i.e. HDO) at lower water vapor concentrations.²⁵ Alternative peak processing techniques that included baseline correction, and integration using Simpson's rule, were also carried out, but determined to be unnecessary. A description of peak processing protocol is provided in the SI. For a set of analyses of a given material, the first 1-2 replicates are discarded due to memory effects imposed by the previous standard or sample, and the latter hydrogen isotope measurements are averaged. Analytical uncertainty is calculated as 1 standard deviation of the mean (1 σ) of a group of averaged replicate measurements. To account for VSMOW scale compression, D/H ratios for samples measured by OA-ICOS are translated into δ D_{VSMOW}, using two-point linear calibrations, developed from reference standards with significantly different δ D values. Slopes and intercepts of calibration regressions were calculated with 95% confidence intervals using GraphPad Prism® statistical software. Calibration equations were then analyzed by ANCOVA in Prism®, to test whether the slopes of lines were equal.

RESULTS AND DISCUSSION

Results for mineral and water standards are presented in Table 2. Mineral analyses, excluding biotite, are accurate within 1.2 ‰ of IRMS-measured δ D_{VSMOW} values, on average. Water standards run through the tube furnace exhibit average accuracy of 1.7 ‰. Biotite δ D_{VSMOW} results, were enriched for deuterium, relative to established values. Excluding biotite, the average precision of OA-ICOS measurements across all material types reported in Table 2 is 1.1 ‰. Kaolinite, muscovite, serpentine, sericite, gypsum, and talc were measured at average precisions ranging from 0.4 to 2.2 ‰, while the analytical uncertainty of biotite ranged from 2.1 to 3.7 ‰. The average uncertainty for analyses of water standards run through the tube furnace was 0.8 ‰. The precision and accuracy of analyses reported here, mark a significant improvement for rapid LAS measurements of hydrogen extracted from solid compounds, with routine precisions comparable to continuous flow IRMS. IRMS labs typically measure δ D in hydrous solids with uncertainties of 2 ‰, or better.^{15-16,33} For comparison, 5 measurements of organic materials and gypsum in an earlier proof of concept OA-ICOS paper were reported with 1 σ uncertainties ranging from 2 to 5 ‰.²⁵

Routine calibration

Representative calibration plots for minerals and waters are presented in Figure 3. For water standards introduced as pulses from the WVISS (Figure 3, center panel), calibration to the VSMOW scale (δ D_{expected} = slope \times D/H_{measured} + intercept) was not statistically different from minerals (Figure 3, left panel) run during the same timeframe (P=0.61). The calibration equation for water standards run in silver crimped silver capillary tubes (Figure 3, right panel) differed with a steeper slope and lower intercept, relative to both minerals and waters introduced as vapor pulses. In a run that included both silver tube water and mineral standards, the slope of the regression defined by minerals (δ D_{expected} = 6738691 \pm 98772 \times D/H_{measured} - 1041 \pm 14) was statistically different (P<0.001) from the line defined by water capsules (δ D_{expected} = 7607035 \pm 47476 \times D/H_{measured} - 1164 \pm 7). This offset in calibration translates into a decrease in accuracy of \sim 3 ‰, when minerals are calibrated using silver tube water standards, or vice versa. Although less accurate for calibrating minerals, crimped silver tube waters provide a means to analyze high salinity fluid samples. The tube furnace used in this study is less susceptible to salt blockage than septa-based injection systems,³⁴ and nebulizer units (i.e. WVISS). In the experimental setup used here, 1-2 μ L of brine, run as a set of 4-6 crimped silver tubes, may be analyzed in 15 minutes, or less.

Operators wishing to calibrate phyllosilicates with reference waters should run these as vapor pulses directly through the furnace, using the WVISS unit, or comparable vaporization hardware. A one point standardization procedure, developed using the WVISS, provided δD calibration that was accurate to within 2.3 ‰ of δD_{VSMOW} values measured externally by IRMS, for analyses of minerals with values ranging from -23.8 to -81.4 ‰. However, moderate scale compression was observed for materials significantly outside this range, highlighting the need for two point calibration lines (Figure 3) in most applications.

Recommendations for analyzing biotite and other Fe-bearing minerals

Biotite minerals were measured at lower precision and accuracy relative to other results reported here. The OA-ICOS δD_{VSMOW} result for NBS 30 of -52.3 ‰, is significantly more positive than the offline IRMS value of -65.7 ‰.³² This finding, in which OA-ICOS results indicate a more deuterium-enriched hydrogen isotope composition than corresponding offline IRMS measurements, has previously been documented for continuous flow IRMS systems.³⁵ In a recent compilation of analyses of NBS 30 by six TC/EA IRMS labs, the average value was -53.4 ‰,³³ which is comparable to the OA-ICOS value reported here.

Although the causes of positive δD_{VSMOW} anomalies in measurements of biotite by OA-ICOS are not definitively known, it has been postulated that in hot continuous flow extractions, high-Fe biotite (e.g. NBS 30) can impede analyte transfer.^{33,35} With TC/EA systems, full conversion from H_2O to H_2 is inhibited by the formation of isotopically-depleted metal hydrides,³⁵ which impose a deuterium-enriched signature on the analyte hydrogen gas. While we do not rule out metal hydride formation in our analytical setup, we also propose oxidation of Fe by H_2O as a potential cause for unexpectedly positive δD_{VSMOW} measurements in biotite, relative to established IRMS values.³⁶⁻³⁷ In a set of heating experiments, the δD_{VSMOW} signature of water released from NBS 30 at temperatures between 973 and 1073 °C, ranged from -25 to -51 ‰, while δD_{VSMOW} of byproduct H_2 gas ranged from -218 to -256 ‰.³⁶ Any H_2 gas generated by reduction of H_2O in the presence Fe is effectively lost in the OA-ICOS method because the analyte measured is water vapor.

Remnant Fe compounds in the reaction column may impose a reducing effect during several subsequent analyses. This occurred when the Misasa sericite standard was measured following NBS 30. We analyzed the sericite standard 7 times. During the first 4 analyses, the memory effect from NBS 30 was discernable. Results of the final three analyses of Misasa were similar to IRMS values. We report a mean of -57.5 ± 1.6 ‰, which is comparable to reported IRMS values, which range from -56.0 to -59.1 ‰.³⁸

Complications associated with fractionation during mineral dehydration appear to be restricted to biotite. This is an issue that will collectively need to be addressed by users wishing to measure biotite and other Fe-rich minerals using online high temperature dehydration systems coupled with LAS units. Crushing biotite, and other iron-bearing samples to smaller grain sizes has been demonstrated to increase accuracy with TC/EA analyses.^{33,35} With continuous flow OA-ICOS, finer mineral powders may facilitate more rapid dehydration, minimizing fractionation in the hot column. Mixing biotite powders with an oxidant (e.g. CuO), may also minimize reduction of waters evolved from high Fe samples. Memory associated with remnant Fe can be eliminated by cleaning the quartz liner in the dehydration column after biotite analyses.

Sample mass requirements

A yield function was developed by analyzing a kaolinite standard (Kga-1b), over a range of masses. Kga-1b has an established water content of 13.7 ‰.³⁹ Mineral water content, calculated from dry mineral mass, correlated linearly with H_2O peak area for aliquots of kaolinite between 1.80 to 4.80 mg (Figure 4, left panel). This range corresponds with sample water volumes between 0.25 and 0.66 μL H_2O .

Precise and accurate δD_{VSMOW} measurements were recorded for water concentrations from 0.25 to 0.55 μL (Figure 4, right panel). This range of water volumes correlates with H_2O peak maxima in the OA-ICOS analyzer between 6,305 and 14,094 ppmv. The 0.66 μL (4.8 mg) kaolinite analysis in Figure 4 generated a peak water concentration of 16,870 ppmv. This peak is significantly above the concentration correction range for this study, which spanned from 3,000 to 13,500 ppmv (SI). Although mineral powders were typically analyzed at masses equivalent to 0.4 to 0.5 μL H_2O , the yield test presented here indicates that routine analyses can be performed using as little as 0.25 μL H_2O . Accurate concentration correction should be possible for smaller peaks between 3,000 and 6,000 ppmv, which coincide with water pulses of approximately 0.1 to 0.2 μL .

Sample drying tests

Effective removal of adsorbed and interlayer water in clays is a necessary treatment step prior to analyzing the hydrogen isotope signature of structural hydroxyl.⁴⁰⁻⁴² The efficacy of drying techniques for δD analyses of clays is a topic of ongoing discussion in the isotope geochemistry community.⁴⁰⁻⁴² Here, two drying approaches were compared for serpentinite (WS-1), muscovite (G-18502), kaolinite (Kga-1b), and a crushed whole rock sample (BB42) from the Martha Gold Mine, Waihi, NZ (Table 3). The crushed sample is from an interval of drill core, containing illite and smectite clays. In the first approach, materials were dried at 110 °C in a conventional oven for 24 hours.⁴¹ In approach 2, samples powders were dried at 190 °C in a vacuum oven for 5 hours.⁴² The yield function in Figure 4 was used to calculate the mineral structural water weight percent for these tests.

For muscovite, kaolinite, and serpentinite, water content varied by 0.3 weight percent, or less, from established mineral values, regardless of drying treatment. However, for the powdered whole rock sample (BB42), the drying approach significantly impacted results. For BB42, drying for 24 hours at 110 °C in a conventional oven resulted in a 53 percent decrease in H_2O yield. Vacuum oven treatment resulted in a 57 percent decrease in H_2O yield, and provides a more rapid preparation approach that effectively minimizes the interference of interlayer and adsorbed water upon the isotopic signal of hydroxyl.

The broadness of peaks, expressed as a ratio of area / height (Table 3), correlated with established mineral thermal dehydration curves.⁴³ For kaolinite, serpentinite, and the illite-smectite rock powder (BB42), peak dimensions were similar. These materials typi-

cally undergo full dehydration below 700 °C. Peaks for muscovite, and other micas, are characteristically broader than the clays assessed. For muscovite, the majority of weight loss occurs above 500 °C.⁴³ While it was possible to analyze muscovite at 140 second intervals, talc samples dehydrated more slowly, and were analyzed at 12 minute intervals to allow for water concentrations in the analyzer to return to a low baseline. Normal talc retains hydroxyl up to 730 °C, and dehydration continues up to 930 °C.⁴³

The analyses presented in this work, were conducted between 950 and 1000 °C, but the column temperature should be adjusted to suit the analytical needs of the user. For measurements of muscovite, biotite, and talc, a hotter column may be desirable in order to achieve more rapid water extraction. During the course of the study, sulfur compounds condensed at the base of the column and at the first inline filter, where temperatures were below 150 °C. The sulfur is sourced from hydrothermal rock powders (i.e. BB42, Table 3), and anhydrite, which accumulated in the column during gypsum analyses. Although thermal decomposition of sulfate in anhydrite is not predicted to occur at 1000 °C, the reaction can proceed at lower temperatures in the presence of additives, including silica and kaolinite.⁴⁴ The quartz column, liner, and silica wool packing may have enabled this. For many clays, and hydrous sulfates, operating at temperatures below 900 °C may be advantageous.

CONCLUSIONS

In this work, we provide a rapid means to measure the hydrogen isotope composition in minerals by OA-ICOS. Our setup successfully measured water liberated from phyllosilicate and hydrous sulfate minerals at volumes as low as 0.25 µL, at greater precision and speed than has been reported previously for continuous flow LAS measurement of gypsum hydration water.²⁵ High precision was maintained, while running sets of replicates at 140 second intervals, at an effective rate of 6 samples in an hour. This throughput is comparable to, or slightly faster, than modern TC/EA IRMS systems. The analytical setup also provides a straightforward means to analyze high salinity fluids, encased in crimped silver tubes. When compared with IRMS, and recent continuous flow CRDS-based work,²⁶ the run setup, calibration, and maintenance times are significantly shorter for the OA-ICOS protocol outlined here. The methodology presented in this paper is also less expensive than IRMS, and may be implemented for less than \$100,000 USD at list prices for the analytical instrumentation, preparation line, and data processing software. Ultimately, because the hardware is straightforward to maintain, and operation costs are low, this method should allow more individuals and institutions to measure hydrogen isotope ratios in minerals and bulk geologic samples. In particular, assessment of δD signals in minerals is of interest in the mining and geothermal industries, yet is infrequently utilized outside of academic venues due to the cost and time associated with analyses.

ASSOCIATED CONTENT

Supporting Information

SI_ACS_MeringBarker: supplementary text: HDO concentration correction and peak integration (PDF)

SI_ACS_Data_MeringBarker: data processing example, calibrated isotope results (Excel)

AUTHOR INFORMATION

Corresponding Author

*Phone: +64 02108801685. Email: johnmering@gmail.com

ACKNOWLEDGMENT

Funding for this project was provided by a MBIE research grant. Reference materials were contributed by John Dilles (Oregon State), Kurtis Kyser (Queen's), and Haiping Qi (USGS). Robert Van Hale (Otago) performed IRMS verification of hydrous minerals. Peter Jarman, provided technical assistance with construction and maintenance of hardware.

REFERENCES

- (1) Taylor, Jr., H. P. *Econ. Geol.* **1974**, *69*, 843–883.
- (2) Marumo, K.; Nagasawa, K.; Kuroda, Y. *Earth Planet. Sci. Lett.*, **1980**, *47*, 255–262.
- (3) Criss, R. E.; Taylor, H. P. *Geological Society of America Bulletin*, **1983**, *94*, 640–663.
- (4) Giggenbach, W.F. *Earth Planet. Sci. Lett.*, **1992**, *113*, 495–510.
- (5) Marumo, K.; Hattori, K. *Geochim. Cosmochim. Acta*, **1999**, *63*, 2785–2804.
- (6) Alt, J. C.; Shanks, W. C. *Earth Planet. Sci. Lett.*, **2006**, *242*, 272–285.
- (7) Vennemann, T. W.; O'Neil, J. R. *Geochim. Cosmochim. Acta*, **1996**, *60*, 2437–2451.
- (8) Criss, R. E.; Taylor, H. P. *Reviews in Mineralogy*. **1986**, *16*, 373–424.
- (9) Nesbitt, B. E. *SEG Newsletter*. **1996**, *27*, 1–13.
- (10) Barker, S. L. L.; Dipple, G. M.; Hickey, K. A.; Lepore, W. A.; Vaughan, J. R. *Econ. Geol.* **2013**, *108*, 1–9.
- (11) Capuano, R. M. *Geochim. Cosmochim. Acta*, **1992**, *56*, 2547–2554.
- (12) Schimmelmann, A.; Sessions, A. L.; Mastalerz, M. *Annu. Rev. Earth Planet. Sci.*, **2006**, *34*, 501–533.
- (13) Bigeleisen, J.; Perlman, M. L.; Prosser, H. C. *Anal. Chem.* **1952**, *24*, 1356–1357.
- (14) Coleman, M. L.; Shepherd, T. J.; Durham, J. J.; Rouse, J. E.; Moore, G. R. *Anal. Chem.* **1982**, *54*, 993–995.

- (15) Vennemann, T. W.; O'Neil, H. C. *Chem. Geol.* **1993**, *103*, 227–234.
- (16) Sharp, Z. D.; Atudorei, V.; Durakiewicz, T. *Chem. Geol.* **2001**, *178*, 197–210.
- (17) Barker, S. L. L.; Dipple, G. M.; Dong, F.; Baer, D. S. *Anal. Chem.* **2011**, *83*, 2220–2026.
- (18) Lis, G.; Wassenaar, L. I.; Hendry, M. J. *Anal. Chem.* **2008**, *80*, 287–293.
- (19) Penna, D.; Stenni, B.; Šanda, M.; Wrede, S.; Bogaard, T. A.; Gobbi, A.; Borga, M.; Fischer, B. M. C.; Bonazza, M.; Chárová, Z. *Hydrol. Earth Syst. Sci.* **2012**, *14*, 1551–66.
- (20) Hodell, D. A.; Turchyn, A. V.; Wiseman, C. J.; Escobar, J.; Curtis, J. H.; Brenner, M.; Gilli, A.; et al. *Geochimica et Cosmochimica Acta.* **2012**, *77*, 352–368.
- (21) Gázquez, F.; Mather, I.; Rolfe, J.; Evans, N. P.; Herwartz, D.; Staubwasser, M.; Hodell, D. A. *Rapid Commun. Mass Spectrom.* **2015**, *29*, 1997–2006.
- (22) Evans, N. P.; Turchyn, A. V.; Gázquez, F.; Bontognali, T. R. R.; Chapman, H. J.; Hodell, D. A. *Earth Planet. Sci. Lett.* **2015**, *430*, 499–510.
- (23) Gázquez, F.; Calaforra, J. M.; Evans, N. P.; Hodell, D. A. *Chem. Geol.* **2017**, *452*, 34–46.
- (24) Affolter, S.; Fleitmann, D.; Leuenberger, M. *Climate of the Past.* **2014**, *10*, 1291–1304.
- (25) Koehler, G.; Wassenaar, L. I. *Anal. Chem.* **2012**, *84*, 3640–3645.
- (26) Bauska, T. K.; Walters, G.; Gázquez, F.; Hodell, D. *Anal. Chem.* **2017**, *in press*.
- (27) Los Gatos Research. www.lgrinc.com.
- (28) Baer, D. S.; Paul, J. B.; Gupta, M.; O'Keefe, A. In *Diode Lasers and Applications in Atmospheric Sensing*; Fried, A., Ed.; SPIE-The International Society for Optical Engineering: Bellingham, WA. **2002**, 4817, 167–176.
- (29) Gupta, P.; Noone, D.; Galewsky, J.; Sweeney, C.; Vaughn, B. H. *Rapid Commun. Mass Spectrom.* **2009**, *23*, 2534–2542.
- (30) IAEA Reference Sheet for International Measurement Standards: VSMOW2, SLAP2. https://nucleus.iaea.org/rpst/Documents/VSMOW2_SLAP2.pdf
- (31) Werner, R.; Brand, W. *Rapid Commun. Mass Spectrom.* **2001**, *15*, 501–519.
- (32) IAEA Reference Sheet for International Measurement Standards: NBS-30. https://nucleus.iaea.org/rpst/Documents/NBS28_NBS30.pdf
- (33) Qi H.; Coplen, T. B.; Gehre, M.; Vennemann, T. W.; Brand, W. A.; Geilmann, H.; Olack, G.; Bindeman, I. N.; Palandri, J.; Huang, L.; Longstaffe, F., J. *Chemical Geology.* **2017**, *467*, 89–99.
- (34) Skrzypek, G.; Ford, D. *Environ. Sci. Technol.* **2014**, *48*, 2827–2834.
- (35) Qi, H.; Coplen, T. B.; Olack, G. A.; Vennemann, T. W. *Rapid Commun. Mass Spectrom.* **2014**, *28*, 1987–1994.
- (36) Laurent, S.; Lécuyer, C.; Martineau, F.; Robert, F. *Central European Geology.* **2011**, *54*, 81–93.
- (37) Richet, P.; Bottinga, Y.; Javoy, M. *Annual Review of Earth and Planetary Sciences.* **1977**, *5*, 65–110.
- (38) Zhang, L. Ph.D. Dissertation, Oregon State University. **2000**.
- (39) Pruett, R. J.; Webb, W. L. *Clays and Clay Minerals.* **1993**, *41*, 514–519.
- (40) Bauer, K. K.; Vennemann, T. W. *Chemical Geology.* **2014**, *363*, 229–240.
- (41) Lonero, A. Geology Department, Utah State University. Personal communication. **2017**.
- (42) VanDeVelde, J. H.; Bowen, G. B. *Rapid Commun. Mass Spectrom.* **2013**, *27*, 1143–1148.
- (43) Nutting, P. G. *USGS Numbered Series.* **1943**, 197-E, 197–217.
- (44) Swift, W. M.; Panek, A. F.; Smith, G. W.; Vogel, G. J.; Jonke, A. A. *Argonne Natl. Lab.* **1976**, *122*.

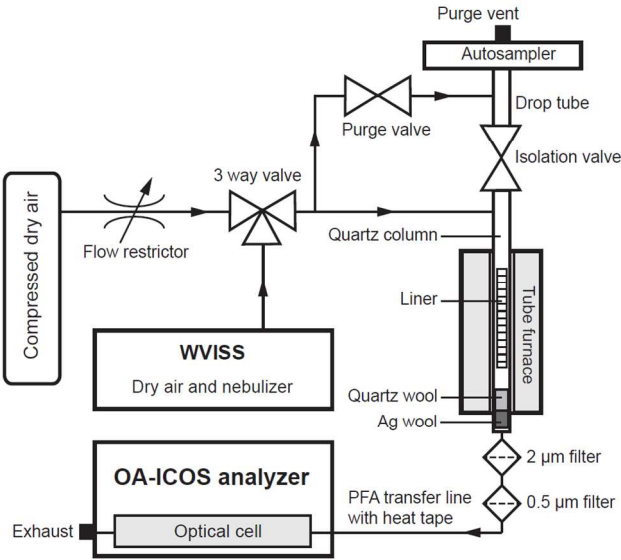


Figure 1. Hardware setup of the mineral dehydration line and LGR OA-ICOS analyzer used for measurement of D/H signatures in hydrous minerals at the University of Waikato. Minerals were dehydrated in a quartz tube, heated to 1000 °C.

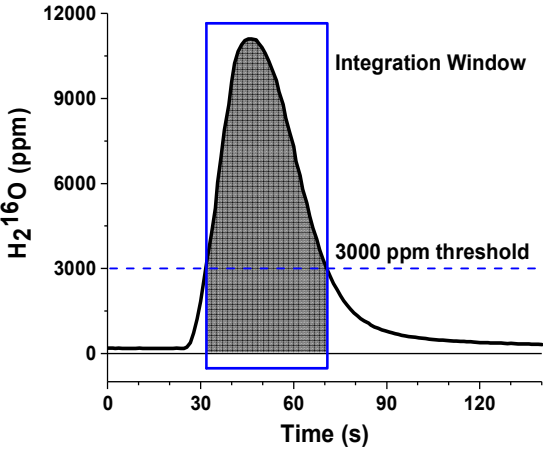


Figure 2. Isotopologue peak areas were integrated in order to calculate isotope ratios (D/H) for samples. Integration was carried out using a water vapor concentration trigger of 3,000 ppmv, and no baseline, for both $H_2^{16}O$ and HDO .

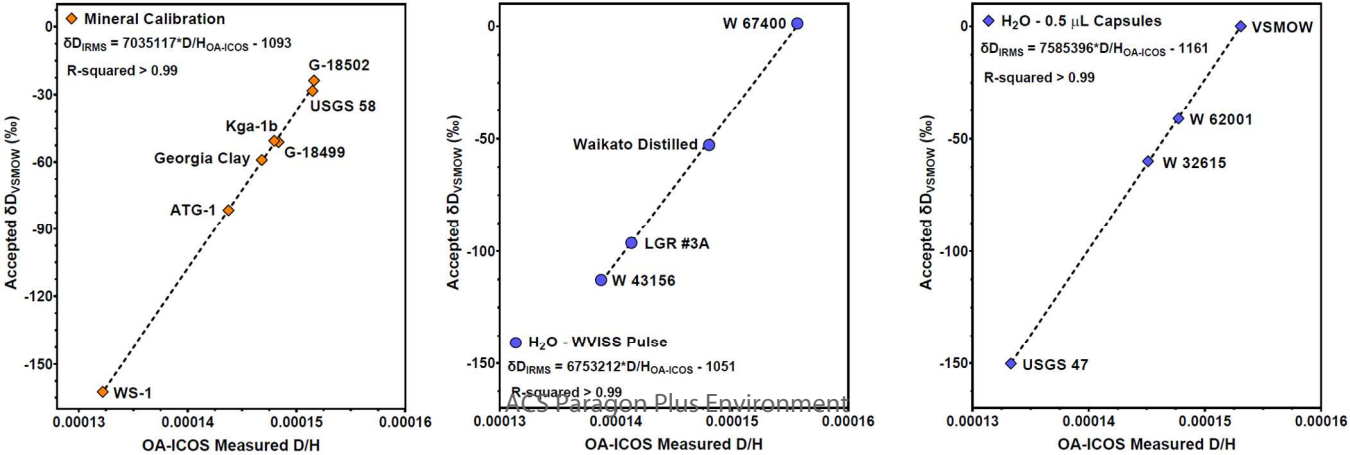


Figure 3. Representative calibration lines. Left panel: Mineral calibration developed from 7 standards measured by IRMS that include serpentine, kaolinite, and muscovite. A highly linear calibration relationship for H₂O liberated from these minerals indicates that these materials may be used interchangeably. Water standards were introduced into the reaction column either as pulses from the WVISS (center panel), or in sealed silver capillary tubes (right panel). The relationship for water pulses from the WVISS is similar to the mineral-based calibration. A small matrix effect associated with water capsules in sealed tubes results in a steeper calibration line (right panel).

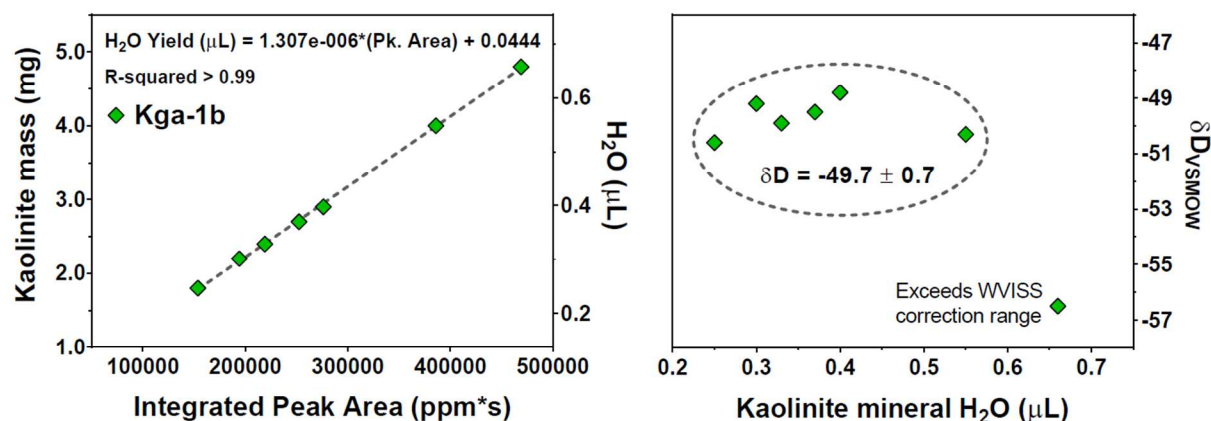


Figure 4. Left panel: yield relative to integrated peak area for the Kga-1b kaolinite standard. A linear relationship facilitates calculation of H₂O content in samples. Right panel: the relationship between sample water content and hydrogen isotope ratio for the Kga-1b kaolinite standard ($\delta D_{IRMS} = -50.5 \%$). Accurate results were obtained for analyses across a range of water volumes evolved from kaolinite. The highest value is above the WVISS concentration correction range. Kga-1b yield standards were dried for 5 hours at 190 °C in a vacuum oven.

Table 1. Materials measured by OA-ICOS in this study

Standard	Type	IRMS δD_{VSMOW}
Hydrous mineral		
G-18502	Muscovite	-23.8
USGS 58	Muscovite	-28.4
Talc-1	Talc	-41.6
G-18499	Muscovite	-51.1
Kga-1b	Kaolinite	-50.5
Georgia Clay	Kaolinite	-59.0
MISASA	Sericite	-59.1
NBS 30	Biotite	-65.7 (-53.4) ^a
ATG-1	Serpentine	-81.4
USGS 57	Biotite	-91.5

1	BuD 96014	Biotite	-158.4
2	Serp-HS-1	Serpentine	-135.3
3	WS-1	Serpentine	-162.4
4	Gy-Ajax	Gypsum	-
5	Gy-HS-1	Gypsum	-
6	BB42	Rock pulp	-
7	H₂O – 0.5 µL silver capsules		
8	VSMOW	Water	0.0
9	USGS W 62001	Water	-41.1
10	USGS W 32615	Water	-60.0
11	USGS 47	Water	-150.2
12	GISP	Water	-189.7
13	H₂O – pulses via WVISS		
14	USGS W 67400	Water	1.2
15	Waikato Distilled	Water	-52.8
16	LGR #3A	Water	-96.4
17	USGS 43156	Water	-112.8

^a The original offline IRMS value of NBS 30 is -65.7 ‰.³²
The updated value by TC/EA-IRMS is -53.4 ‰.³³

Table 2. Analytical results for hydrous minerals and small volumes of water

Standard	δD IRMS	OA-ICOS δD result	1σ	n	Run time	Calibration standards
Serpentine						
Serp-HS-1	-135.3	-134.3	1.6	5	140 s	WS-1, G-18502
WS-1	-162.4	-160.6	1.0	5	140 s	ATG-1, USGS 58
Kaolinite						
Kga-1b	-50.5	-49.7	0.7	6	140 s	WS-1, G-18502
	-50.5	-51.9	1.9	7	140 s	ATG-1, USGS 58
	-50.5	-50.8	1.0	8	140 s	WS-1, G-18502
	-50.5	-50.2	2.2	6	140 s	WS-1, G-18502
	-59.0	-58.0	1.5	6	360 s	ATG-1, USGS 58
Georgia Clay	-59.0	-60.4	0.4	3	140 s	ATG-1, USGS 58

Muscovite							
G-18502	-23.8	-27.5	0.9	4	140 s	ATG-1, USGS 58	
G-18499	-51.1	-49.9	0.4	3	140 s	ATG-1, USGS 58	
	-51.1	-51.4	1.7	3	140 s	WS-1, G-18502	
Sericite							
Misasa	-59.1	-57.5	1.6	3	360 s	ATG-1, USGS 58	
Biotite							
NBS 30	-53.4	-52.3	2.1	3	360 s	ATG-1, USGS 58	
USGS 57	-91.5	-82.8	3.3	5	360 s	ATG-1, USGS 58	
BuD96014	-158.4	-148.0	3.7	5	360 s	ATG-1, USGS 58	
Talc							
Talc-1	-41.6	-44.1	1.2	2	720 s	Waikato Distilled	
	-41.6	-40.0	1.9	2	720 s	Waikato Distilled	
Gypsum							
Gy-Ajax	-	-62.7	1.3	4	360 s	ATG-1, USGS 58	
Gy-HS-1	-	-114.5	1.2	4	360 s	ATG-1, USGS 58	
H₂O - 0.5 µL Ag capsules							
VSMOW	0.0	-2.7	0.3	4	360 s	W 32615, USGS 47	
W 62001	-41.1	-40.7	1.0	5	360 s	VSMOW, USGS 47	
W 32615	-60.0	-60.6	1.0	6	360 s	VSMOW, USGS 47	
	-60.0	-61.9	1.0	4	360 s	VSMOW, USGS 47	
GISP	-189.5	-191.5	1.0	5	360 s	W 32615, USGS 47	
H₂O - WVISS pulse via column							
Waikato Distilled	-52.8	-50.0	0.6	7	180 s	W 67400, W 43156	
LGR #3A	-96.4	-95.2	0.6	3	180 s	W 67400, W 43156	

^a The original offline IRMS value of NBS 30 is -65.7 ‰.³² The updated value by TC/EA-IRMS is -53.4 ‰.³³

Table 3. Assessment of mineral drying techniques by OA-ICOS

Mineral	Treatment	H ₂ O (wt. %)	1σ	H ₂ O Area (ppmv×s)	H ₂ O Max (ppmv)	Area / Height	D/H (×1E-04)
WS-1 (serpentine) H ₂ O = 12.2 % ^a	No drying	12.4	0.2	299003	11186	26.7	1.325
	24 hrs at 110 °C	12.2	0.5	290967	10883	26.7	1.314
	5 hrs at 190 °C, vacuum	12.1	0.2	282312	10594	26.6	1.320
Kga-1b (kaolinite) H ₂ O = 13.7 % ^b	No drying	13.7	0.2	329589	12208	27.0	1.471
	24 hrs at 110 °C	13.4	0.2	317902	11819	26.9	1.472
	5 hrs at 190 °C, vacuum	13.7	0.4	323548	11944	27.1	1.476
BB42 (crushed rock)	No drying	11.5	0.3	480021	17047	28.2	1.472

1	<i>illite / smectite</i>	24 hrs at 110 °C	5.4	0.1	256436	9507	27.0	1.427
2		5 hrs at 190 °C, vacuum	4.9	0.7	233691	8720	26.8	1.441
3	G-18502 (muscovite)	No drying	-	-	391854	11610	33.8	1.523
4	H ₂ O = 4.3 % ^a	24 hrs at 110 °C	4.1	0.0	382672	10989	34.8	1.518
5		5 hrs at 190 °C, vacuum	4.2	0.0	399230	11563	34.5	1.518
6	^a Calculated from TC/EA results, University of Otago							
7	^b Pruett and Webb, 1993							
8								
9								
10								
11	Table of Contents (TOC) graphic							
12								
13								
14								
15								
16								
17								
18								
19								
20								
21								
22								
23								
24								
25								
26								
27								
28								
29								
30								
31								
32								
33								
34								
35								
36								
37								
38								
39								
40								
41								
42								
43								
44								
45								
46								
47								
48								
49								
50								
51								
52								
53								
54								
55								
56								
57								
58								
59								
60								

